COMPLEX REFLECTION COEFFICIENTS APPLIED TO STEEP SLOPING STRUCTURES

FRITZ BÜSCHING

Prof. Dr.-Ing., Bielefeld University of Applied Sciences, Hydromech, Dießelhorststr.1, 38116 Braunschweig, Germany, buesching@hollow-cubes.de

Abstract

Based on lab investigations, specific phenomena of waves breaking on rather steep slopes (1:2 and 1:3) are traced back partly to varying phase shifts $\Delta\varphi$, occurring between incident and reflected waves. As an analogue of electromagnetic waves at uniform planar interfaces, the process of wave breaking is regarded as combined effects resulting from reflection, transmission and dissipation. Accordingly, a complex reflection coefficient Γ is defined comprising of the magnitude $C_r = H_r / H_i$ and the phase $\Delta\varphi$. Results are presented by magnitudes and phases for irregular waves in the *complex number plane* and for monochromatic waves with reference to some frequencies and slope angles.

1. Introduction

The effects of breaking waves are decisive for the design of coastal structures. As far as sloping structures are concerned, the breaker number ξ, also termed Ir (after Iribarren, 1949), has proved to be the most useful parameter.

$$\xi = \tan\alpha / \sqrt{(H/L)} \qquad [1]$$

Its variables are the slope angle $\tan\alpha$ = 1:m , wave height H and wave length L.
As is well known, this parameter is used not only for classifying the different types of breakers but also for describing the reflectivity of structures by using the ratio of reflected wave height divided by incident wave height (H_r / H_i), which normally is termed reflection coefficient.

By contrast, the effect of phase shifting γ between incident and reflected wave, presumed already by (Schoemaker and Thijsse ,1949), did not draw very much attention. The author, however, had come across this phenomenon, when investigating breaking waves at different revetment structures producing a phase jump $\Delta\varphi$ (Büsching, 2010).

Previously Sutherland and O´Donoghue, (1998) analysed the state of knowledge from about 20 references complementing it by their own experiments. Using an extensive experimental data set, involving normal incident and oblique incident regular and irregular waves, they arrived at the conclusion that the phase shift γ is uniquely determined by a nondimensional number χ_3 defined by structure slope $\tan\alpha$ = 1:m, water depth at the structure toe d_t , wave period T, and angle of incidence θ.

$$\chi_3 = \chi\sqrt{\cos\theta} = \frac{1}{\tan\alpha}\sqrt{\frac{d_t \cos\theta}{gT^2}} \quad . \qquad [2]$$

Accordingly neither the wave height nor energy dissipation processes should influence the phase shift, with the consequence that such quantities were irrelevant for the description of breaking waves too.

The author, however, has arrived at more differentiated results, regarding the breaking process of waves at rather steep sloping structures in such a way that a variable phase difference $\Delta\varphi$ between the incident and reflected wave plays an important part in the reflection process (Büsching, 2010).

In the author's view not only the phenomena of reflection and dissipation have to be considered for describing the wave breaking process, but transmission too; just like an analogue of electromagnetic waves at uniform planar interfaces: In the course of the dissipating wave breaking process, a wave pulse of transmission evolves from the initial incident wave at the landward side, while a reflected wave is produced on the seaward side at the same time. The wave pulse of transmission is characterized by a wave height $H_t < H_i$ and phase velocity $c_t < c_i$, and the reflected wave height is $H_r < H_i$. In this process it is essential that due to the conservation of momentum, the positive water level deflection of the transmitted wave pulse postulates locally a negative water level deflection of the reflecting wave. Hence, the superimposition of incident and reflected waves results in a partially standing wave comprising of a phase jump $\Delta\varphi$. The partial clapotis node close to the point IP, where the structure front face intersects the still water level, can be regarded as a center of nearly elliptical movement, around which the water level deflections of the washing movement (runup – rundown) and those of the partial standing wave occur in opposite (flipping) phases, see Figure 1

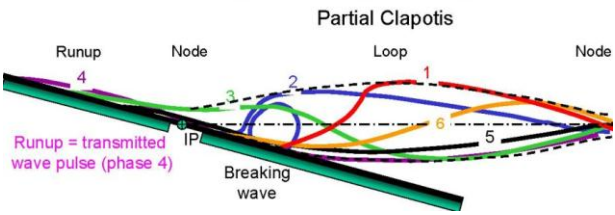

Figure 1. Six phases of a plunging breaker at the condition of a phase jump, caused by partial reflection and by the transmitted pulse of wave run up. In phases 3 and 4, there are opposite water level movements (flipping deflections) at both sides of the node nearly coinciding with IP.

The trigger of the author´s above considerations is due to the findings, derived from wave tank tests executed on hollow concrete elements in the wave tank of Bielefeld University of Applied Sciences (BUAS) in the 1990ies, see Figure 2.

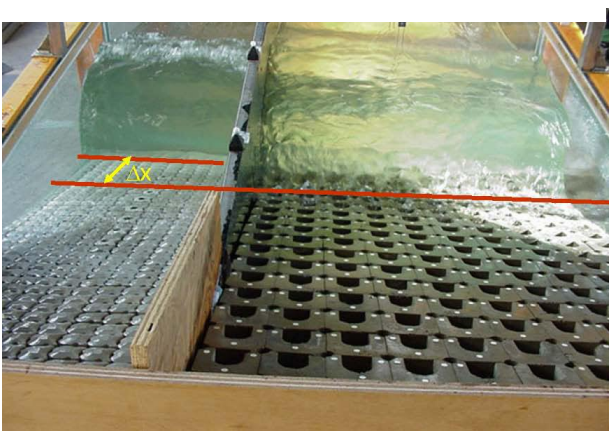

Figure 2. Plunging breaker at quasi smooth reference revetment slope 1:3 (left) and collapsing breaker at hollow slope structure 1:3 (right). Varying distances (Δx) between breaker front faces indicate modified phase shifts between incident and reflected waves.

Especially such tests of scale 1:5 have shown that by means of appropriate interference with the washing movement not only the wave run-up and the breaker height could significantly be reduced, but also the breaker type and its relative position on the slope face was modified (Büsching, 1992).

The following results, presented in (Büsching, 2010) regarding the occurrance of a phase jump, will be partly extended and modified respectively. Therefore, instead of defining the reflection

coefficient as a function of two variables $C_r = f(H_r/ H_i, \Delta\varphi)$, it will be defined as a complex quantity $\Gamma = C_r e^{i\Delta\varphi}$, which appears to be the more appropriate option.

For the time being, however, linkages to the results of the above mentioned studies of Sutherland und O´Donoghue, (1998) cannot be made, because in the present assessment

- the point IP of the still water level intersecting the slope face is selected as the point of reference and thus the phase shift here is $\Delta\varphi \neq \gamma$,
- the investigations are restricted to the 2-dimesional retro-reflection from 4 (2 x 2) steep slopes only,
- contrary to above presumptions essential importance is attached to the interactions between phase shift and energy dissipation at wave breaking and
- absorption at sloping structures is assumed to be not only represented by a smaller reflecting wave height $H_r < H_i$ but also is accompanied by a modified phase shift $\Delta\varphi$ between incident and reflected wave.

2. Mathematical Pre-examinations

In the general case of regular monochromatic waves the mathematical formulation of the incident wave with amplitude A can be given as follows:

$$y(x,t) = A\cos(\omega t - kx) = Re[A\cos(\omega t - kx) + i\,A\sin(\omega t - kx)]$$

$$= Re\left[Ae^{i(\omega t - kx)}\right] = Ae^{i(\omega t - kx)} \qquad [3]$$

where the angular frequency $\omega = \frac{2\pi}{T}$ and the wave number is $k = \frac{2\pi}{L}$.

The expression of the reflected wave results from the incident wave by multiplying the later by the reflection coefficient and thereby accounting for a phase shift $\Delta\varphi$. Moreover, a negative sign has to be used at the wave number, because the reflected wave moves in the opposite direction. If the place of reflection is supposed to be at x=0, which is located at the right hand side, the wave activity is in the negative range and the description of the reflected wave is as follows:

$$y(x,t) = C_r A\cos(\omega t + kx + \Delta\varphi) = C_r \cdot Ae^{i(\omega t + kx + \Delta\varphi)}$$

$$= (C_r e^{i\Delta\varphi}) \cdot Ae^{i(\omega t + kx)} = \Gamma \cdot Ae^{i(\omega t + kx)} \qquad [4]$$

According to equation (4) capital gamma Γ is defined as a complex reflection coefficient (in short: CRC), i.e. complex reflected wave divided by the complex incident wave, - related to x = 0

$$\Gamma = C_r e^{i\Delta\varphi} \qquad [5]$$

where $C_r = H_r/ H_i$ is the wave height ratio and $\Delta\varphi$ is the phase shift (phase difference) between the reflected and the incident wave at the point of reflection.
Consequently the total wave field can be formulated by summing up equations [3] and [4] in the cosine formulation as

$$y(x,t) = Acos(\omega t - kx) + C_r Acos(\omega t + kx + \Delta\varphi) \quad [6]$$

and in the polar complex vector presentation as

$$y(x,t) = Ae^{i(\omega t - kx)} + C_r Ae^{i(\omega t + kx + \Delta\varphi)} = (e^{-ikx} + C_r e^{i\Delta\varphi} e^{ikx}) Ae^{i\omega t}$$

$$= (e^{-ikx} + \Gamma\, e^{ikx}) Ae^{i(\omega t)} \quad [7]$$

Besides other purposes equation [7] also forms the basis for the design of electronic communication devices. Its evaluation gives the following two special cases of total reflection:

Positive total reflection

$$y(x,t) = (e^{ikx} + e^{-ikx}) Ae^{i\omega t} = 2\, Acos\, kx\, e^{i\omega t} \quad [8]$$

where $\Delta\varphi = 0°$ and $C_r = 1$ then $\Gamma = 1$.

This is the equation of a perfect standing wave without phase jump.

Negative total reflection

$$y(x,t) = (e^{-ikx} - e^{ikx}) Ae^{i\omega t} = -2\, i\, Asin\, kx\, e^{i\omega t} \quad [9]$$

where $\Delta\varphi = 180°$ and $C_r = 1$ then $\Gamma = -1$.

This is also the equation of a perfect standing wave, however, with a phase jump of 180° (π) between incident and reflected wave. Both standing waves are shifted one against the other in position by L/ 4 and in phase by 90°.

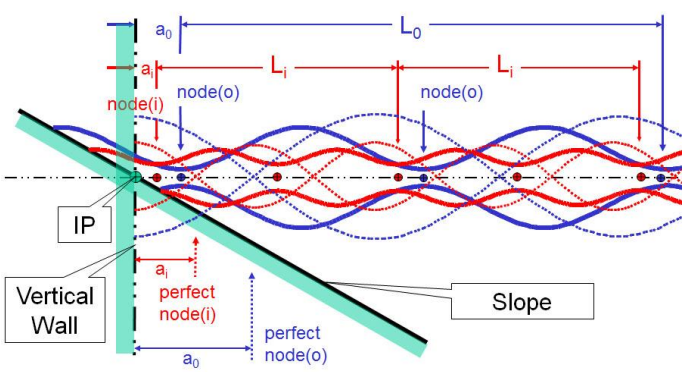

Figure 3. Two sets of (partial) standing waves of lengths L_o and L_i at a vertical wall (total reflection; dotted lines) and at a slope (partial reflection; solid lines). Pure surging wave not shown. Node distances $a = \eta_{min}$, see Figure 4.

As it is well known, both cases also appear approximately when generating standing rope waves in a single vertical plane. If the rope is not fixed at its rear end in the vertical direction, there is positive total reflection, whereas negative total reflection exists, if the rope is fixed at the rear end in both vertical and horizontal directions.

Until recently, at water waves the case of positive total reflection had been specified only, namely as a *Clapotis* at a vertical wall, see Figure 3. Considering the vertical wall as the *one* special case of *reflection from an inclined plane*, however, the *second* case of negative total reflection can be recognized as an ideal *surging wave* from a smooth inclined plane. In reality, however,

approximate versions of both cases are possible only, resulting in partial standing waves assigned by positive or negative reflection respectively.
By contrast to the authors former definition of a reflection coefficient as a function of two variables $C_r = f(H_r / H_i, \Delta\varphi)$, which can be named a reflection coefficient sui generis (Büsching, 2010), the complex reflection coefficient (in short: CRC) $\Gamma = C_r e^{i\Delta\varphi}$ comprises the complete definition instead of the common use of the wave height ratio $C_r = H_r / H_i$ only.

3. Experimental Procedure for the Determination of Complex Reflection Coefficients

It is well known that reflection coefficients can be determined from measurements on the wave field. In the case of water waves, however, until recently the structure of Healy´s formula (1953) was used for the determination of the magnitude of the reflection coefficient $C_r = H_r / H_i$ only.

$$C_r = \frac{H_{max} - H_{min}}{H_{max} + H_{min}} \quad \text{where} \quad H_{max} = H_i + H_r \text{ and } H_{min} = H_i - H_r \qquad [10]$$

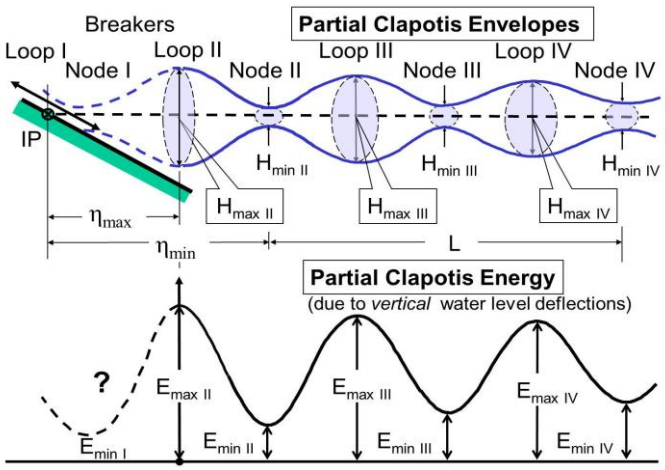

Figure 4. Sketch of water level envelopes derived from the potential energy of a partial standing wave at a slope, based on wave energy spectrum measurements at BUAS-Laboratory since 1992

In this equation the quantities H_{max} and H_{min} refer to the vertical distances of the partial Clapotis envelopes shown in the upper part of Figure 4.
In the case of irregular waves, the author, however, since 1992 keeps on using the following formula [11], which is modified from Healy´s in such a way that the sums and differences of the wave heights of formula [10] had been substituted by the square roots of the energy´s extreme values, to be taken from the lower part of Figure 4.

$$C_{r,i} = \frac{\sqrt{E_{max,i}} - \sqrt{E_{min,i}}}{\sqrt{E_{max,i}} + \sqrt{E_{min,i}}} \quad . \qquad [11]$$

where:
$E_{max,i}$ = maximum energy of contributing frequency components at clapotis node i,
$E_{min,i}$ = minimum energy of contributing frequency components at clapotis node i,
i = ordinal number of partial clapotis loops or nodes respectively.

With respect to the phase shift $\Delta\varphi$, however, *hardly any analysis* of extensive water level deflections of partial standing waves has been executed, since Mansard and Funke (1980) had introduced their 3-point method for separating irregular incident and reflected waves.

Besides the above maximum and minimum water level deflections or values of energy respectively, especially for the determination of the reflection coefficient´s phase (CRC Phase),

additionally the wave length L and the distance η between the effective reflection point and an (imperfect) loop or node respectively are needed, see Figure 4.

If the distance between the reflection point and the nearest loop is known, the phase of the reflection coefficient can derived from the following consideration.

Assuming a spot (on a wave train) at a distance η from the reflection point, the phase shift for the incident wave to travel from here up to the point of reflection is $k\eta = 2\pi(\eta/L)$. At the point of reflection the (unknown) phase shift Δφ appears and the thereby reflected wave needs another kη to return to the initial spot.

Thus at this spot, the total phase difference between incident and reflected wave has summed up to yield $2k\eta + \Delta\varphi$. At the condition of a loop existing at the respective spot, this phase difference must be an integer multiple of 2π, so that incident and reflected waves superimpose to give maximum water level deflections.

Hence, this can be put in the following equation

$$2k\eta_{max} + \Delta\varphi = n \cdot 2\pi \qquad [12]$$

With n = 1 for the nearest loop to the reflecting structure this equation can be solved for the phase angle Δφ of the reflection coefficient:

$$\Delta\varphi = 2\pi - 2k\eta_{max} \qquad \text{respectively}$$

$$\Delta\varphi[°] = 360\left(1 - \frac{2\eta_{max}}{L}\right) \qquad [13a]$$

With regard to the condition of a node, the respective phase difference must be equal to an odd integer multiple of 180° (π), in order that incident and reflected waves tend to cancel.

Hence, the analogue formula is

$$\Delta\varphi[°] = 180\left(1 - \frac{4\eta_{min}}{L}\right) \qquad [13b]$$

While in (Büsching, 2010) the primary focus had been put on slopes 1:3 (Figure 2), in the present study the findings regarding the phase of the complex reflection coefficient (CRC-Phase) at the slopes 1:2 will be discussed in detail, because of the tremendous differences between the two kinds of revetment.

The respective measurements had been carried out by Lemke und Nicolai (1998) and evaluations and conclusions had been presented by Büsching (1999). As to be seen from Figure 5 in this case two layers of a special kind of big hollow cubes had been piled up in such a way that a stepped permeable structure was formed. Corresponding to the investigations on slope 1:3, the point IP of the still water level intersecting the slope face was selected as point of reference. Hence in this case synchronous measurements of water level deflections had been possible above the smooth slope starting at a distance of 10cm from IP and above the hollow block structure starting directly at IP. The total measurements extended up to the distance of 3.1m from the structure quasi synchronously at gauge stations intervals of 10cm.

Differing from the investigations on slopes 1:3, in this case truncated wave sequences had been applied in such a way that re-reflection and resonance effects were excluded from the analyzed data. Instead of plotting the energy data of any partial wave separately, in Figure 6 the energy of all partial waves, comprising different component frequency ranges, appear piled up with reference to the distance from IP.

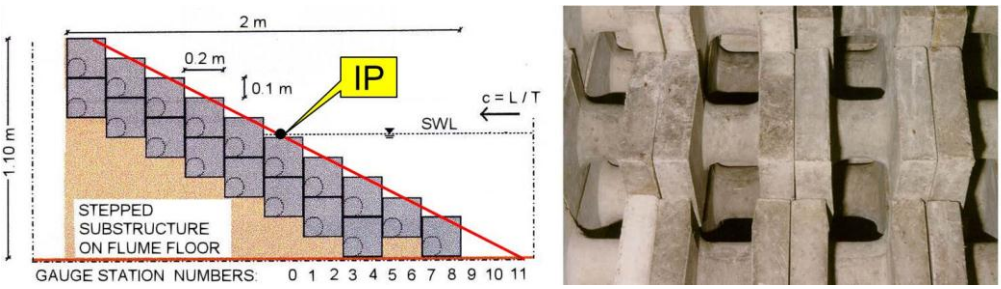

Figure 5. Sectional view and cut-out view of the permeable test structure versus a smooth slope inclined 1:m = 1:2 (Red line intersecting the still water level = IP).

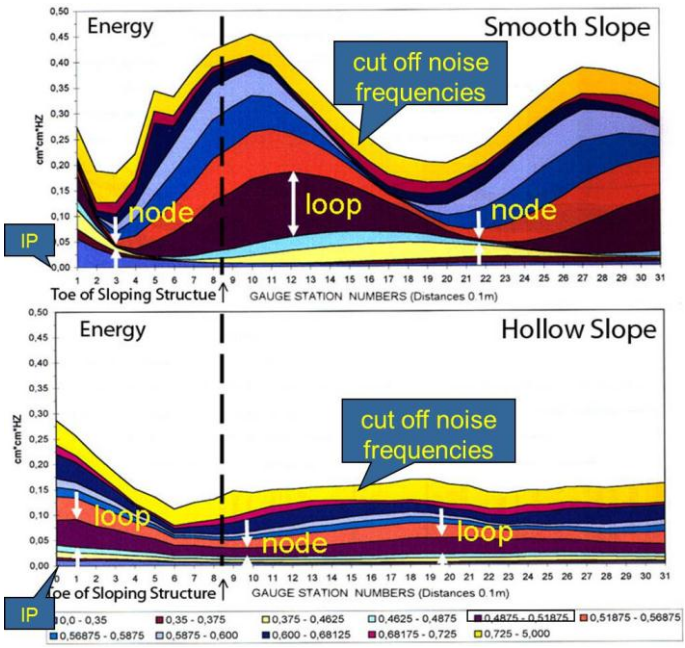

Figure 6. Energy content of 11 frequency ranges with the distance from IP. Upper part: Evidence of partial standing wave components (partial waves) assigned by distinct loops and nodes. Lower part: Evidence of partial waves containing much less energy. Both parts: Distinct phase differences $\Delta\psi$ between partial waves of same frequency ranges.

Omitting signal noise of frequencies $f > 0.725$ Hz (i.e. the upper yellow-orange areas in both plots), at the smooth slope, partial waves can very well be identified by their extreme values of energy, representing loops and nodes respectively. It is to be seen that the lower the frequency components of the partial waves, the more downslope they are reflected with the consequence of the relative shifting to be seen in the graph.

At this place, the approach, however, is concentrated on the tremendously different amounts of energy in front of the two slopes and also on the existence of the big phase differences $\Delta\psi$ between respective component partial waves. By way of example with regard to the frequency range $0.4875\text{Hz} \le f \le 0.51875\text{Hz}$ (purple), whose loops and nodes in the graph are marked by arrows, the distance of corresponding phase points is about 0.70m. Applying 0.95m as the distance between node and loop (also taken from the graph) the phase difference can be determined easily to be approximately $\Delta\psi \approx 66°$.

4. Magnitudes and Phases of Complex Reflection Coefficients

It should be stated that in Figure 7 the magnitudes and phases of the CRC are included for 5 partial waves only, representing the core of the spectrum.

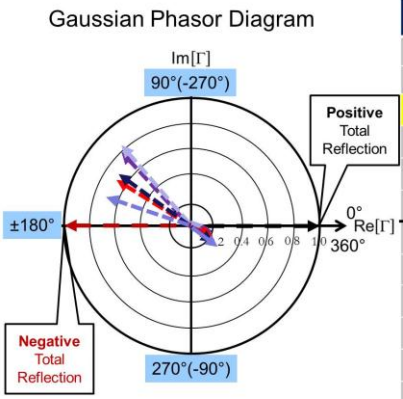

f[Hz]	L[m]	η_{max}[m]	C_r	Δφ[°]
Smooth Slope				
0.475	4.4	1.40	0.83	130.9
0.503	3.8	1.20	0.80	132.6
0.544	3.4	1.00	0.68	148.2
0.578	3.0	0.90	0.69	144.0
0.594	2.9	0.80	0.70	161.4
Hollow Cubes				
0.475	4.4	2.15	0.09	8.2
0.503	3.8	1.95	0.16	-9.5
0.544	3.4	1.80	0.18	-21.2
0.578	3.0	1.65	0.21	-36.0
0.594	2.9	1.60	0.25	-37.2

Figure 7. Phasor diagram basing on the data of the table on the right. The CRC values Γ of the two structures on an average not only differ considerably in magnitude (0.72 > 0.2) but also in phase($\Delta\Delta\varphi \approx 180°$.

While the magnitudes C_r had been calculated by applying equation [11] considering the energy data E_{max} and E_{min} of index II (cf. Figure 4) from Figure 6, the phases Δφ had been calculated from equation [13a] using the respective η_{max} values.

As can be seen from the Gaussian Phasor Diagram, the 5 big phasors of the CRC referring to the smooth slope, are characterized by magnitudes of about $C_r = 0.72$ and frequencies between 0.47Hz and 0.6Hz

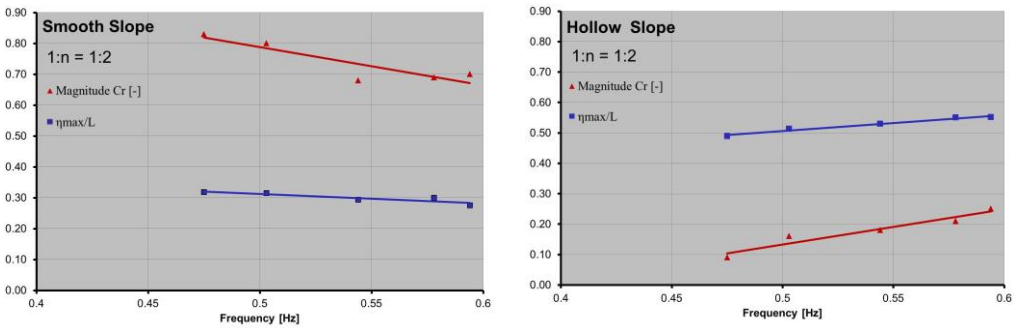

Figure 8. Magnitudes C_r and relative loop distances η_{max}/ L with frequency.

(core of spectrum). They all are in the second quadrant and thus represent negative reflection (Re[Γ]<0). On the other hand the small CRC-phasors referring to the hollow cube structure have magnitudes of about $C_r = 0.2$ and are nearly all in the fourth quadrant, which means positive reflection (Re[Γ]>0). In order to consider the dependence on frequency as well in the data presentation, besides the common subdividing of complex functions into Real Re[Γ] and Imaginary Im[Γ] parts (not shown) in this case also the magnitudes C_r

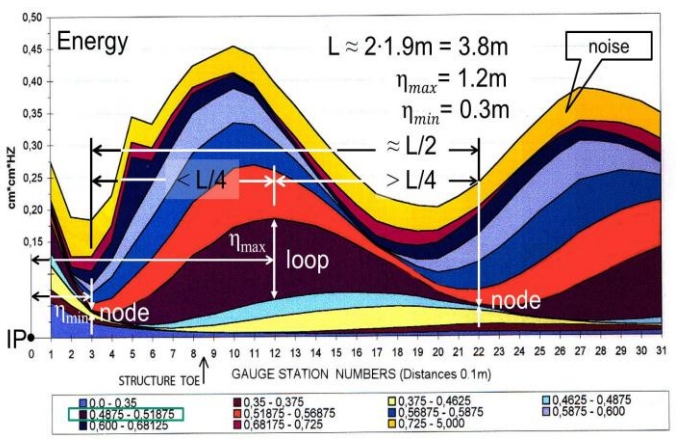

Figure 9. *Horizontal wave asymmetry* due to decreasing distances between loops and nodes in onshore direction, at the smooth slope.

and the relative loop-distances η_{max}/ L can be plotted, see Figure 8.

By judging the accuracy of the data taken from charts like Figure 6, not only the measurement interval of 10cm has to be considered, but also the fact that near breaking steepening waves are deformed continuously, e.g. see (Büsching, 1974). The *horizontal wave asymmetry* is not only expressed by the above described relative shifting of the partial waves, but also by the decreasing distances between loops and nodes of all partial waves in the onshore direction. As an example, in Figure 9 the relevant data are given for the partial wave of the frequency range $0.4875Hz \leq f \leq 0.51875Hz$ (purple). Hence, the formulae [13a] and [13b] yield different results even for neighboring loops and nodes at a smooth slope. In this case $\Delta\varphi = 132.6° > 123.2°$, to be compared to the respective value in the table of Figure 7. This means that not only CRC magnitudes vary with distance from the structure (as stated by Büsching, (1992) but also the CRC phases do so.

5. Conclusions

Including the CRC magnitudes C_r and the CRC phases $\Delta\varphi$ of Figure 10, which had been derived from data of (Büsching, 1995), and results from (Büsching, 2010), it can be stated that

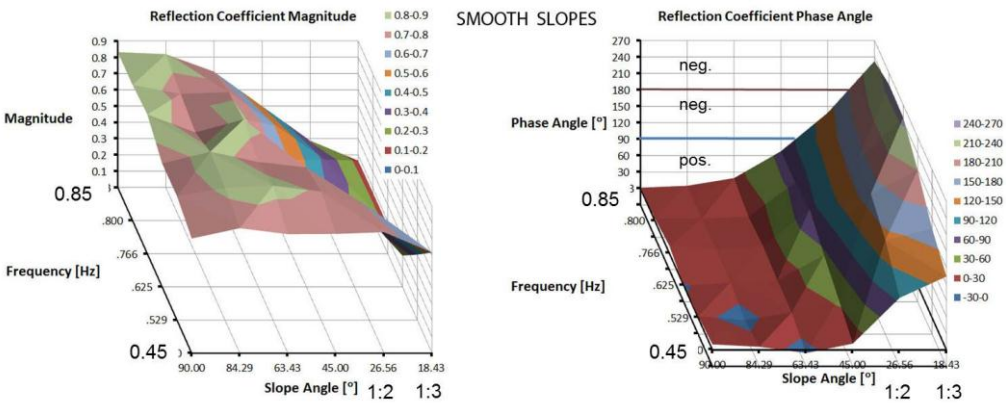

Figure 10: CRC Magnitudes and Phases of 6 smooth revetments, inclined 90°, 84,29°, 63,43°, 45°, 26,56° and 18,3° for monochromatic waves, covering the frequency range $0.45Hz \leq f \leq 0.853$ Hz. Magnitudes calculated by using equation [11] and phases by equation [13b].

- there is an opposite trend between magnitudes and phase angles with respect to the slope angle axis, i.e. the phase angles increase with decreasing slope angles
- and there is also an opposite trend between magnitudes and phase angles with respect to the frequency axis for slope angles $1:3 \leq 1:n \leq 1:1$ ($18,43° \leq \alpha \leq 45°$), i.e. the phase angles decrease with decreasing frequencies f (or increasing wave lengths L respectively).

Phase angle $\Delta\varphi$	Type of breaker	Further condition
≈ 0°	broken **Clapotis**	super critical steepness
1st or 4th quadrant (positive reflection)	no distinct breaker type	dissipation>transmission
≈ 180°	**surging** breaker	low dissipation
2nd or 3rd quadrant (negative reflection)	collapsing or plunging breaker	dissipation and transmission

Moreover, the table on the left contains observed types of breakers related to CRC phase angles.

Finally it can be stated:

As the *CRC phase angle* controls the positioning of the partial standing wave and thus the location of the breaker depth at a slope, its necessity for the complete description

of the *wave breaking* is obvious and therefore it should be considered for future large scale investigations. Nevertheless it should be emphasized that due to the small sample size, general conclusions on the *breaker type* depending on the kind of reflection cannot be given at present. On the other hand such results can be expected in future, if targeted investigations will not only be oriented at the magnitudes but also at the corresponding phase data of complex reflection coefficients,- both maybe related to Irribarren numbers. In doing so, especially the nature of the high scatter in the CRC magnitudes C_r with respect to Irribarren numbers $0.3 \leq \xi \leq 9$ (van der Meer, 1988) can possibly be clarified.

The use of complex reflection coefficients is another example of phenomena, known from electromagnetic and other kinds of waves, having particular significance for water waves too. It may be speculated that an all-in approach of corresponding complex coefficients on *reflection, transmission and absorption* could be useful.

Due to the limited space available, it is not possible to discuss the complete results in detail. An extended English version exists at http:/ / www.digibib.tu-bs.de/ ?docid=00045344 .

References

Büsching, F. 2012. 'Komplexe Reflexionskoeffizienten für Wasserwellen', *Die Küste*, H.79 (2012) in printing.

Büsching, F. 2010. 'Phasensprung bei der partiellen Reflexion irregulärer Wasserwellen an steilen Uferböschungen', *BINNENSCHIFFFAHRT - C 4397 D, 65*,H.9 p.73-77 & H.10 p.64-69, 2010.

Büsching, F. 2010. 'Phase Jump due to Partial Reflection of Irregular Water Waves at Steep Slopes', 1. *Coastlab10*, Barcelona, 28th-30th September, 1st October 2010, Paper No. 67,p.1-9.

Büsching, F. 2001. 'Combined Dispersion and Reflection Effects of Sloping Structures', *International Conference on Port and Maritime R&D and Technology ICPMRDT*, P.411-418, Singapore, 29.-31.10.2001, Proc./ CD.

Büsching, F. 1999. 'Reflection from Hollow Armour Units', Proc. *COPEDEC V*, p.1362 - 1370, Cape Town, South Africa.

Büsching, F. 1995. 'Hollow Revetment Elements', *Proc. Fourth International Conference on Coastal and Port Engineering in Developing Countries COPEDEC IV*, Rio de Janeiro, S. 961-976, 1995.

Büsching, F. 1992. 'Wave and Downrush Interaction on Sloping Structures' *Proc. 10th International Harbor Congress, Antwerpen*, S. 5.17-5.25, 1992

Büsching, F. 1974. 'Über Orbitalgeschwindigkeiten irregulärer Brandungswellen', *Mitteilungen des Leichtweiß-Instituts für Wasserbau der TU Braunschweig*, H.42, p. 0 - 256.

Lemke, S. und Nicolai, A. 1998: ‚Reflexion an einer aus Beton-Hohlformkörpern (Hollow Cubes) bestehenden Böschung mit der Neigung 1:2', *Diplomarbeit FH Bielefeld University of Applied Sciences*, 1998, unpublished.

Mansard, E.P.D. and E.R. Funke. 1980. 'The Measurement of Incident and Reflected Spectra Using a Least Squares Method'. *17th International Conference on Coastal Engineering, Sydney*, 23-28 March, 1980.

Schoemaker, H.J. and J.Th. Thijsse. 1949. 'Investigation of the reflection of waves', *Third Meeting, Intern. Assoc. Hyd. Structures Res.*, 1-2 September, 1949

Sutherland, J. and O'Donoghue, T. 1998 'Wave Phase Shift at Coastal Structures', *Journal of Waterway, Port, Coastal and Ocean Engineering*, Vol. 124, No. 2, March/ April 1998, pp. 90-98.

Van der Meer, J.W. 1988.'Rock slopes and gravel beaches under wave attack'. *Doctoral thesis. Delft University of Technology. Also Delft Hydraulics Communication* No. 396.